Excitation Function for the ^{74}Se(^{18}O,*p*3*n*) Reaction

J. M. Gates[1,2,*], I. Dragojević[1,2], J. Dvorak[1], P. A. Ellison[1,2], K. E. Gregorich[1], L. Stavsetra[1] and H. Nitsche[1,2]

[1] *Nuclear Science Division, Lawrence Berkeley National Laboratory, Berkeley, CA 94720, USA*
[2] *Department of Chemistry, University of California, Berkeley, Berkeley, CA 94720, USA*

Production of ^{88g}Nb/^{74}Se(^{18}O,p3n)/Excitation function/Berkeley Gas-filled Separator (BGS)

Summary

The ^{74}Se(^{18}O,*p*3*n*)^{88g}Nb excitation function was measured and a maximum cross section of 495±5 mb was observed at and ^{18}O energy of 74.0 MeV. Experimental cross sections were compared to theoretical calculations using the computer code ALICE-91 and the values were found to be in good agreement. The half-life of ^{88g}Nb was determined to be around 14.56±0.11 min.

1. Introduction

The study of the chemistry of transactinide elements (Z ≥ 104) is a topic of great interest in current nuclear chemistry research. Experiments focus on comparing the chemical properties of transactinide elements to those of theirs lighter homologues [1]. However, transactinides can only be produced one atom-at-a-time through nuclear reactions and will exist at the microscopic scale in any chemistry technique. To best replicate the chemical conditions under which the transactinide elements are studied, it is necessary to study the lighter homologues at concentrations low enough that there are no

interactions between homologue ions. In this work, we report on the measurement of the ^{74}Se(^{18}O,p3*n*) excitation function to produce short-lived ^{88g}Nb for use in group five homologue chemistry experiments.

2. Experimental

Short-lived niobium, ^{88g}Nb was produced at the Lawrence Berkeley National Laboratory's 88-Inch Cyclotron using the ^{74}Se(^{18}O,p3*n*) reaction. At the entrance to the Berkeley Gas-filled Separator (BGS), the ^{18}O beam passed through a (40-45) μg/cm^2 carbon vacuum window and a negligible amount of helium gas before entering the target. The target consisted of 384-μg/cm^2 ^{74}Se, deposited on 40-μg/cm^2 C and covered with 5-μg/cm^2 Au. The typical beam intensity of the $^{18}O^{4+}$ projectiles was 75 particle·nA.

Energy losses of the ^{18}O beam in C and Au were calculated using SRIM2006.02 [2]. Two PIN diode detectors located at ±27° from the beam axis continuously monitored the product of target thickness and beam intensity by the on-line detection of Rutherford-scattered particles. Systematic uncertainty in the absolute energy from the 88-Inch Cyclotron is estimated to be ~1% [3]. However, relative energies were determined to within 0.1% by analysis of the pulse heights of the Rutherford-scattered projectiles from the various ^{18}O energies. The resulting center-of-target beam energies were 64.0, 68.6, 74.0, 78.9 and 83.9 MeV in the laboratory frame. Compound nucleus excitation energies were calculated using the relative beam energies with the experimental mass defects for ^{18}O, ^{74}Se and ^{88g}Nb [4]. The resulting ranges of compound nucleus excitation energies within the targets were 57.5±0.5, 61.1±0.5, 65.5±0.5, 69.4±0.5 and 73.4±0.5 MeV.

The niobium evaporation residues (EVRs) recoiling out of the target were separated in the BGS from the beam and most unwanted reaction products based upon their differing magnetic rigidities in the 67-Pa He of the BGS [5, 6]. The magnetic rigidity for the niobium EVRs were estimated as previously described [3] and experimentally determined to be 0.95 T·m. The efficiency for collecting ^{88}Nb EVRs at the BGS focal plane was modeled using a Monte Carlo simulation of the EVR trajectories in the BGS, as described earlier [3, 7], and resulted in efficiencies (ε_{BGS}) of 36-44%, depending on the beam energy.

The recoiling atoms were slowed down by passing through a 3.3-μm Mylar window, after traveling through the BGS, at the entrance to the 40 mm-deep Recoil Transfer Chamber (RTC) [8, 9]. In the RTC, the EVRs were then thermalized in approximately 1.3 bar of helium gas. Helium gas at flow rates of 1.6 - 1.8 L/min was seeded with potassium chloride aerosols, produced in an oven at a temperature of 650°C, before entering the RTC. The EVRs were captured on the aerosols and transported through a 2-mm i.d. and ~20 meter long stainless steel capillary to the chemistry setup where they were deposited on small platinum foils at the exit of the gas-jet capillary. Figure 1 contains a schematic of the experimental setup.

To measure the half-life of ^{88}Nb, the aerosols were collected for 30 – 45 minutes and then dissolved in 3 mL dilute hydrochloric acid (HCl). The 3 mL aliquots where then assayed using a HPGe γ–detector and counting intervals of 3 min. Four parallel experiments were performed and the spectra from each counting interval were summed.

For measurement of the ^{74}Se(^{18}O,p3n)^{88}Nb excitation function, the aerosols were collected for ten minutes and subsequently dissolved in 3 mL dilute HCl. The 3 mL

aliquot was then assayed for four minutes on a HPGe γ-ray detector. Corrections were made for decay during collection, decay during counting, γ-ray intensities and efficiencies of the gas-jet, BGS and HPGe γ-ray detector.

3. Results and Discussion

3.1 ^{88g}Nb half-life

The half-life of ^{88g}Nb has been measured several times in other works, leading to values of 14.4±0.2 min [10] 14.3±0.3 min [11] and 13.3±1.0 min [12]. Figure 2 contains a sample spectrum obtained from the collected reaction products. Lines that are significantly above background are labeled. In addition to the ground state, ^{88}Nb is known to have a metastable state with a 7.7 min half-life and several prominent γ-ray energies (271.80, 671.20, 1057.01 and 1082.53 keV) can be from the decay of both ^{88g}Nb and ^{88m}Nb [10]. However, ^{88m}Nb also contains lines at 262.04, 450.52 and 760.76 keV that are not present in the decay of ^{88g}Nb [10]. As these lines were not observed in any of the spectra from the reaction products, it was determined that contamination in the 271.80, 671.20, 1057.01 and 1082.53 keV lines due to the decay of ^{88m}Nb is negligible.

The ^{88g}Nb half-life was determined from the decay curves fitted to the 271.80, 671.20, 1057.01 and 1082.53 keV lines using first order exponentials, as shown in Figure 3. These fits resulted in a weighted-average half-life of 14.56±0.11 min, which is consistent with and more precise than previous measurements from [10, 11].

3.2 Excitation Function for the ^{74}Se(^{18}O,*p*3*n*)^{88g}Nb Reaction

The excitation function for the ^{74}Se(^{18}O,*p*3*n*)^{88g}Nb reaction is shown in Figure 4 and the resulting cross sections and errors are listed in Table 1. Cross sections for the reaction were calculated using a weighted average of the 271.80, 671.20, 1057.01 and

1082.53 keV γ-ray lines. A maximum cross section of 495±(stat = 5, syst = 205) mb was observed at an ^{18}O energy of 74.0 MeV.

3.3 Systematic Uncertainty of Cross Sections

Systematic uncertainties in the measured cross sections are the result of seven main contributions: i) calculations of the cross sections were performed using the half-life measured in this work (14.56±0.11 min). This value has a 0.8% error, leading to a 1.2% error in the cross section measurement. ii) the uncertainty in the efficiency for transport of EVRs through the BGS and the mylar window and into the RTC. An uncertainty of 10% has been estimated for the transport of EVRs to the focal plane detector for the ^{48}Ca + $^{206\text{-}208}$Pb reactions by a comparison of the size and shape of the modeled and experimental focal plane position distributions [3]. However, since the (Z, A) of ^{88g}Nb is outside the range of the normal operation of the BGS, a more conservative uncertainty of 20% was used. iii) the angle of the Rutherford scattering monitor detectors is known within 0.2° with respect to the beam direction. This results in a 3% uncertainty in the Rutherford scattering cross section, corresponding to a 3% error in the EVR cross sections. iv) the uncertainty in the solid angle subtended by the collimators placed in front of the monitor detectors is dominated by uncertainty in the size of the 4.78 mm opening and is estimated to contribute 4% to the systematic error in cross sections. v) between the target and the Rutherford scattering monitor detectors are a series of screens that attenuate the scattered particles. In the ^{207}Pb(^{48}Ca,2*n*)^{253}No reaction, the ratio of ^{253}No EVRs in the focal plane detector to the Rutherford scattered ^{48}Ca ions was measured with and without the attenuation screens. The uncertainty in the attenuation factor was determined to be 5%. vi) the systematic uncertainty in the absolute energy

from the 88-Inch Cyclotron is ~1%, resulting in energy uncertainties of 0.6 - 0.8 MeV and Rutherford scattering cross section uncertainties of 2%. vii) the gas-jet efficiencies have been measured to 30-70% in the previous experiments [9, 13], although the variation during an experiment has been measured at <5% [14]. We conservatively estimate the gas-jet efficiency to be 50±20%. Standard error propagation of the seven systematic contributions results in a systematic error of ~40%. Statistical uncertainties due to the number of counts observed are 1 - 2%.

3.4 Theoretical Predictions with ALICE-91, EVAPOR and HIVAP

We have compared the experimental cross sections to theoretical predictions from ALICE-91 [15], EVAPOR [16] and HIVAP [17]. The ALICE-91 code calculates equilibrium (EQ) cross sections using the Weisskopf-Ewing model [18]. ALICE-91 was previously found to accurately reproduce the results of reactions between ^{18}O and ^{65,63}Cu when COST = 1.5, a = A/9 and n_0 = 16 [19]. Due to the similarity between the ^{16}O + ^{65,63}Cu and ^{18}O + ^{74}Se reactions, we have chosen to use COST = 1.5 and a = A/9. In this work, n_0 was 18. A comparison of the experimental and theoretical values is shown in Fig. 4. Theoretical values from HIVAP underestimate the experimental cross sections by a factor of 10. HIVAP also predicts that the centroid of the excitation function occurs 10 MeV below the energy obtained experimentally. EVAPOR underestimates the experimental cross sections by a factor of 3 and predicts that the centroid of the excitation function occurs at excitation energies that are 10 MeV higher than those observed experimentally. EVAPOR also predicts a broader excitation function than that observed experimentally. ALICE-91 accurately reproduces the height and width of the experimental excitation function. Similar agreement between experimental

data and theoretical predictions from ALICE-91 were observed in [19] for the *p*x*n* reactions with ^{18}O and ^{65,63}Cu.

4. Acknowledgements

The authors would like to thank the staff of the 88-inch cyclotron at Lawrence Berkeley National Laboratory for providing the ^{18}O beams. The EVAPOR calculations for the ^{18}O-based reactions were carried out by H. Mahmud, whom we gratefully acknowledge. We would also like to thank Ch. E. Düllmann for the HIVAP calculations. This work was supported by the Director, Office of Science, Office of High Energy and Nuclear Physics, Division of Nuclear Physics, US Department of Energy under Contract No. DE-AC02-05CH11231.

5. Disclaimer

6. References

[1] Schädel, M.: Angew. Chem. Intl. Ed. **45**, 368 (2006).
[2] Ziegler, J. F.: Nucl. Instrum. Methods B **219-220**, 1027 (2004).
[3] Gregorich, K. E., Loveland, W., Peterson, D., Zielinski, P. M., Nelson, S. L., Chung, Y. H., Düllmann, C. E., Folden III, C. M., Aleklett, K., Eichler, R., Hoffman, D. C., Omtvedt, J. P., Pang, G. K., Schwantes, J. M., Soverna, S.,

Sprunger, P., Sudowe, R., Wilson, R. E., Nitsche, H.: Phys. Rev. C **72**, 014605 (2005).
[4] Audi, G., Bersillon, O., Blachot, J., Wapstra, A. H.: Nucl. Phys. **A729**, 3 (2003).
[5] Gregorich, K. E., Ninov, V.: J. Nucl. Radiochem. Sci. **1**, 1 (2000).
[6] Ninov, V., Gregorich, K., McGrath, C. A., in *ENAM 98: Exotic Nuclei and Atomic Masses*, edited by B. M. Sherrill, D. J. Morrissey and C. N. Davids (American Institute of Physics, Woodbury, New York, 1998), p. 704.
[7] Gregorich, K. E., Ginter, T. N., Loveland, W., Peterson, D., Patin, J. B., Folden III, C. M., Hoffman, D. C., Lee, D. M., Nitsche, H., Omtvedt, J. P., Omtvedt, L. A., Stavsetra, L., Sudowe, R., Wilk, P. A., Zielinski, P. M., Aleklett, K.: Eur. Phys. J. A **18**, 633 (2003).
[8] Kirbach, U. W., Folden III, C. M., Ginter, T. N., Gregorich, K. E., Lee, D. M., Ninov, V., Omtvedt, J. P., Patin, J. B., Seward, N. K., Strellis, D. A.: Nucl. Instrum. Methods A **484**, 587 (2002).
[9] Kirbach, U. W., Gregorich, K., Ninov, V., Lee, D. M., Patin, J. B., Shaughnessy, D. A., Strellis, D. A., Wilk, P. A., Hoffman, D. C., Nitsche, H.: Lawrence Berkeley National Laboratory Annual Report; (1999).
[10] Oxorn, K., Mark, S. K.: Z. Phys. A **316**, 97 (1984).
[11] Iafigliola, R., Turcotte, R., Moore, R. B., Lee, J. K. P.: Nucl. Phys. A **182**, 400 (1972).
[12] Doron, T. A., Blann, M.: Nucl. Phys. A **161**, 12 (1971).
[13] Düllmann, C. E., Folden III, C. M., Gregorich, K. E., Hoffman, D. C., Leitner, D., Pang, G. K., Sudowe, R., Zielinski, P. M., Nitsche, H.: Nucl. Instrum. Methods A **551**, 528 (2005).
[14] Gates, J. M., Sudowe, R., Ali, M. N., Calvert, M. G., Dragojević, I., Ellison, P. A., Garcia, M. A., Gharibyan, N., Gregorich, K. E., Nelson, S. L., Neumann, S. H., Parsons-Moss, T., Stavsetra, L., Nitsche, H.: Radiochim. Acta (in production).
[15] Blann, M., NEA Data Bank, Gif-sur-Yvette, France, Report No. PSR-146 (1991).
[16] Beene, J. R., Nicolis, N. G.: (unpublished).
[17] Reisdorf, W., Schädel, M.: Z. Phys. A **343**, 47 (1992).
[18] Weisskopf, V. F., Ewing, D. H.: Phys. Rev. **57**, 472 (1940).
[19] Chowdhury, D. P., Guin, R., Saha, S. K., Sudersanan, M.: Nucl. Instrum. Methods B **211**, 288 (2003).

Table 1: Energies and cross sections for the $^{74}Se(^{18}O, p3n)^{88}Nb$ reaction.

Center-of-Target Beam Energy (MeV)	Excitation Energy (MeV)	Cross Section (mb)	Statistical Error (mb)	Systematic Error (mb)
64.0	57.5	325	5	135
68.6	61.1	395	5	160
74.0	65.5	495	5	205
78.9	69.4	375	5	155
83.9	73.4	325	5	135

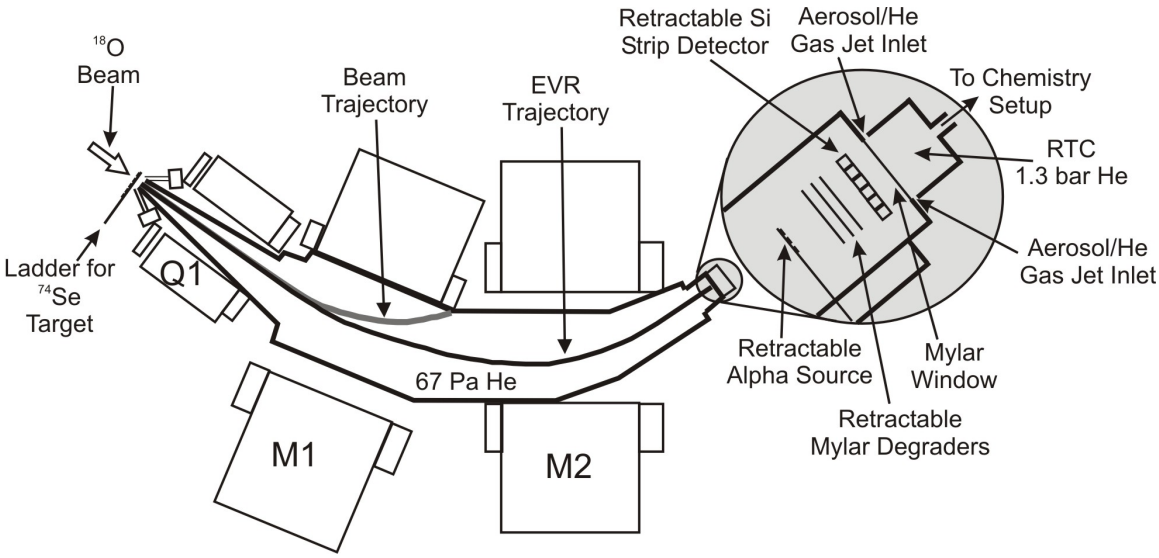

Figure 1: Schematic of the BGS at LBNL in the configuration required for chemistry experiments with preseparation. Q1 is the quadrupole magnet, M1 is a gradient-field dipole magnet and M2 is a flat-field dipole magnet. These magnets provide separation between the EVR's of interest and the beam and other unwanted reaction products. Modified from [13].

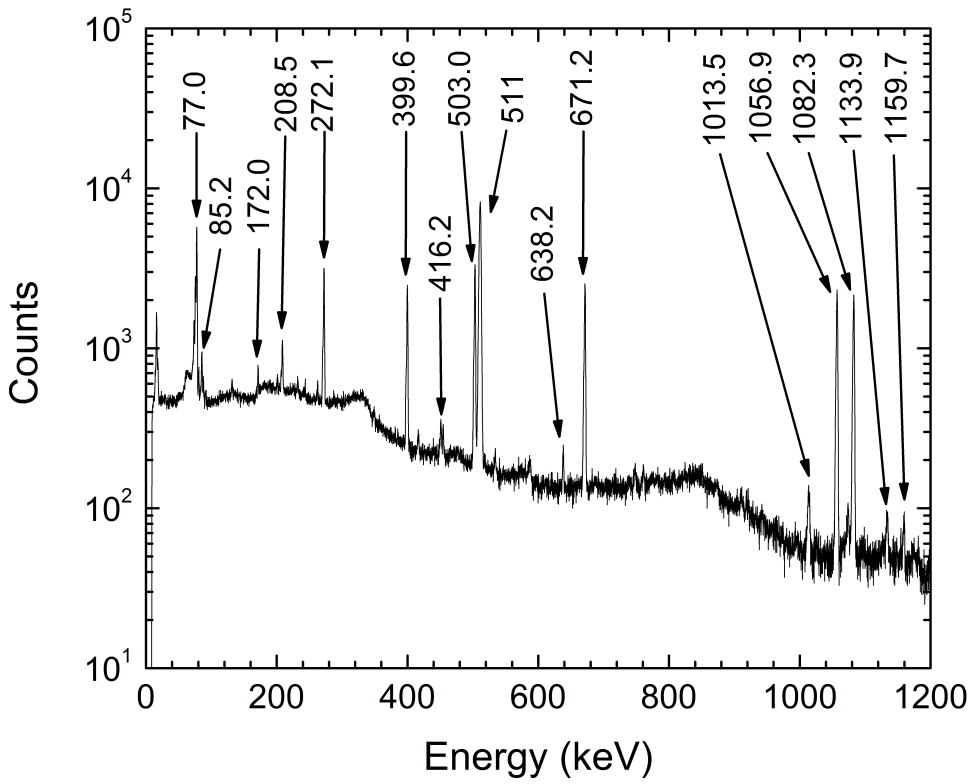

Figure 2: Sample γ-ray spectrum of the recoil products obtained from a bombardment of ^{74}Se with ^{18}O, after separation by the BGS. Lines significantly above background are labeled with their energies in keV.

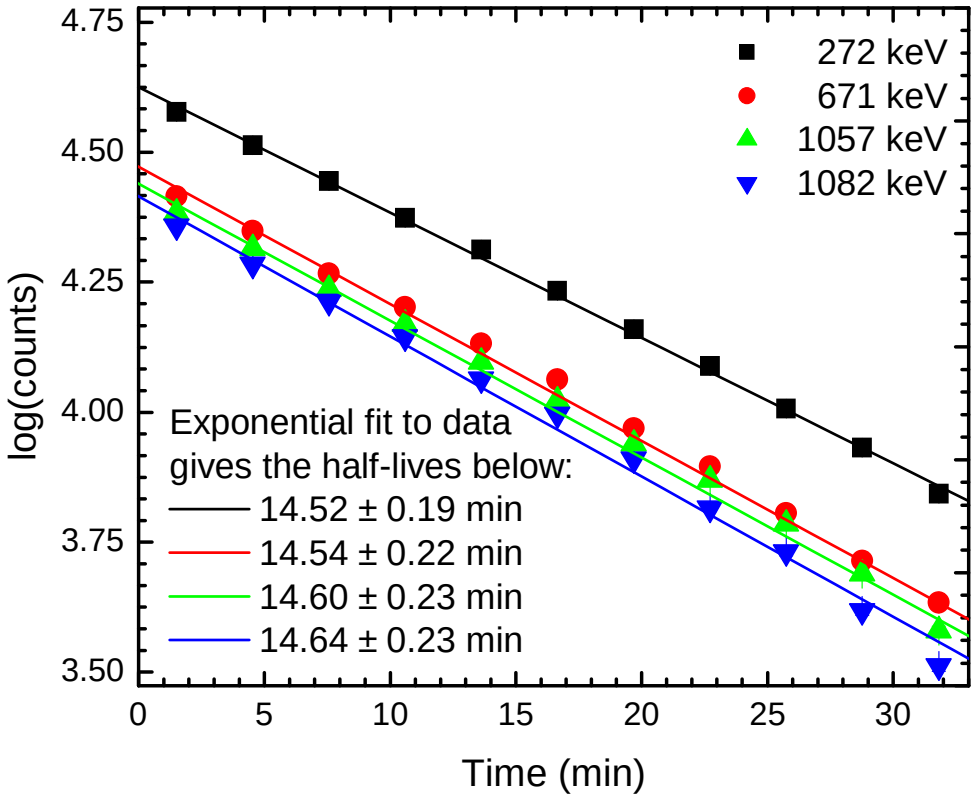

Figure 3: Decay data and exponential fits to the data for the four prominent γ-ray lines. Error bars in the vertical direction are smaller than the symbols.

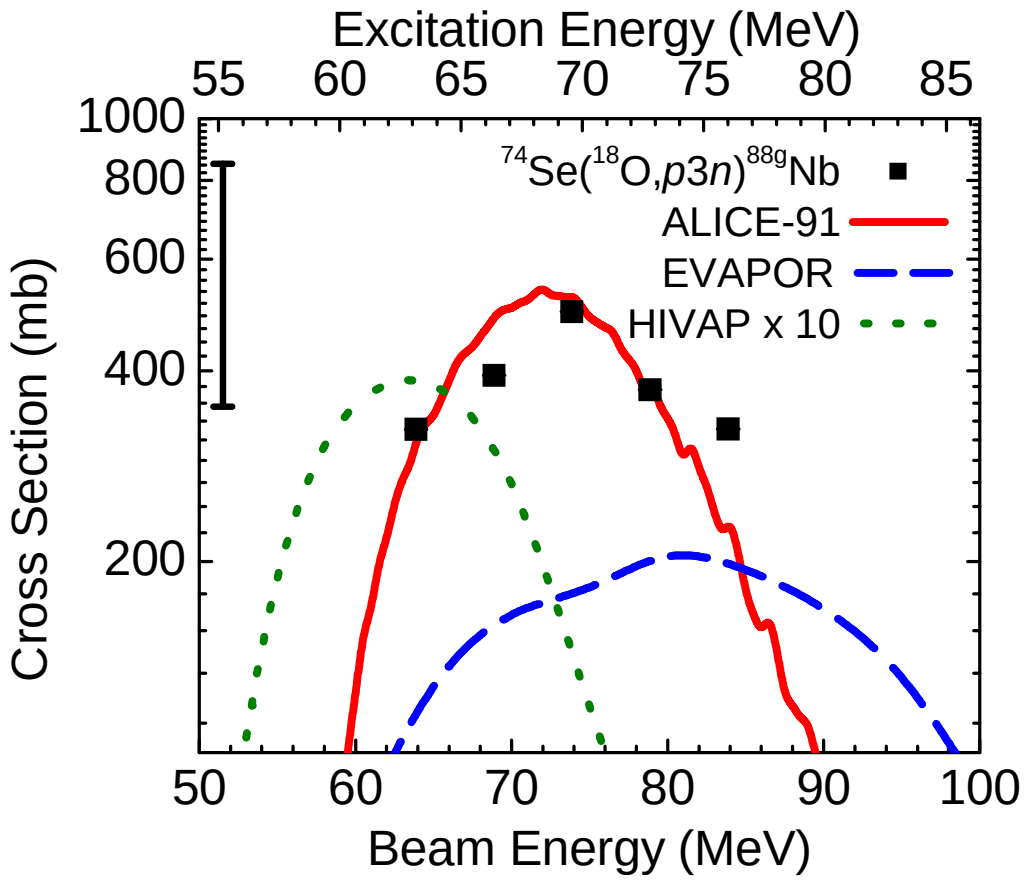

Figure 4: Excitation function for the ^{74}Se(^{18}O, $p3n$)^{88}Nb reaction. The horizontal width of the symbols shows the energy spread of the beam within the target. In the vertical direction, statistical errors are smaller than the size of the symbols. The bar in the upper left-hand corner represents the size of the systematic errors at the 1σ level. Theoretical predictions from ALICE-91, EVAPOR and HIVAP are shown by the solid, dashed and dotted lines, respectively.